

Phase Transformation and Magnetic Properties of La-Ca-Co-Zn Doped M-type Hexaferrites

An Jianzhang¹, Ye Jinwen¹, Tang Zhenghua¹, Chen Yike², Qin Yao³

¹ Sichuan University, Chengdu 610041, China; ² Chengdu Jintai precision Co. Ltd, Chengdu 610041, China; ³ Southwest Petroleum University, Chengdu 610500, China

Abstract: The phase transformation process from 25 °C to 1450 °C and the magnetic properties of $\text{Sr}_{0.3}\text{La}_{0.3}\text{Ca}_{0.4}\text{Fe}_{10.625}\text{Co}_{0.225}\text{Zn}_{0.1}\text{O}_{19}$ were investigated by high-temperature X-ray diffraction, thermal analysis, vibrating sample magnetometer and scanning electron microscopy. The results show that the formation of M-type hexagonal ferrites in air passes through two endothermic reactions. SrCO_3 and partial Fe_2O_3 first generate the intermediate phase $\text{Sr}_3\text{Fe}_2\text{O}_{7-d}$ around 700 °C. And then $\text{Sr}_3\text{Fe}_2\text{O}_{7-d}$ and the remaining unreacted Fe_2O_3 generate $\text{SrFe}_{12}\text{O}_{19}$. Meanwhile, La^{3+} , Ca^{2+} , Co^{2+} and Zn^{2+} ions gradually dissolve in the intermediate phase or the latter product M phase with the temperature increasing. The perovskite was obtained when annealed at about 700 °C, which may transform perovskite into $\text{Sr}_3\text{Fe}_2\text{O}_{7-d}$ during the cooling process. The average valence of Fe in $\text{Sr}_3\text{Fe}_2\text{O}_{7-d}$ is a function of temperature. A very high single degree of M phase and a small number of second phase were obtained at about 1200 °C, and the cationic are evenly distributed in the crystal. The rectangularity of the demagnetizing curves of the LaCaCoZn-type substituted ferrite powder decreases compared to that of unsubstituted ferrite powder. The ferrite will be decomposed at about 1380 °C.

Key words: intermediate phase; phase changes; magnetic properties; thermal analysis

Currently a significant improvement of the magnetic properties of M-type ferrites can be obtained by the partial substitution of Sr^{2+} or Fe^{3+} ions, or both.

Research on the phase transition of magnetoplumbite has a guiding effect on the pre-sintering process of ferrite. Batti^[1] first systematically studied the $\text{SrO-Fe}_2\text{O}_3$ pseudo-binary system, highlighting the strontium-rich phases SrFeO_3 , $\text{Sr}_3\text{Fe}_2\text{O}_7$ and $\text{Sr}_3\text{Fe}_2\text{O}_7$. Later, the pseudo-binary system $\text{SrO-Fe}_2\text{O}_3$ ^[2] and the pseudo-ternary system $\text{CaO-SrO-Fe}_2\text{O}_3$ ^[3], $\text{La}_2\text{O}_3\text{-SrO-Fe}_2\text{O}_3$ ^[4], etc. were also reported. La^{3+} and Ca^{2+} can completely replace Sr^{2+} , but the phase region of $\text{LaFe}_{12}\text{O}_{19}$ and $\text{CaFe}_{12}\text{O}_{19}$ is extremely narrow, the requirement of temperature is high, and it is difficult to prepare. $\text{SrFe}_{12}\text{O}_{19}$ can be stabilized to 1390 °C, and then began to incongruently melt to form $\text{SrFe}_{18}\text{O}_{27}$ and liquid phase. In the study of Batti^[1], SrO did not show solubility in $\text{SrFe}_{12}\text{O}_{19}$. However, it was later found that the proportioning of iron deficiency can

get a single M phase at the appropriate temperature, which indicates that SrO has certain solubility in $\text{SrFe}_{12}\text{O}_{19}$ ^[5,6]. The point is also confirmed by Langhof^[7], showing that the phase width decreases as the temperature decreases and disappears until 1100 °C. At present, there are two main viewpoints about the intermediate phase: Haberey^[8] found that perovskite SrFeO_{3-d} will be generated between 660 °C and 730 °C, then SrFeO_{3-d} with the remaining Fe_2O_3 to generate $\text{SrFe}_{12}\text{O}_{19}$. And Berbenni^[9] also confirmed this in the later study. However, Beretka^[10] found that the intermediate phase obtained in vacuum and air are SrFe_2O_4 and $\text{Sr}_2\text{Fe}_2\text{O}_5$. And the two phases almost appeared at the same time.

In the present study, the formula of the $\text{Sr}_{0.3}\text{La}_{0.3}\text{Ca}_{0.4}\text{Fe}_{10.625}\text{Co}_{0.225}\text{Zn}_{0.1}\text{O}_{19}$ component was prepared by the solid-state reaction method to investigate that reaction process with increasing temperature and magnetic properties.

Received date: August 25, 2018

Foundation item: Sichuan Panxi Strategic Resources Innovation and Development Pilot Area Third Batch of Major Science and Technology Project (CDWA2016ZC3-3)

Corresponding author: Tang Zhenghua, Ph. D., Associate Professor, College of Materials Science and Engineering, Sichuan University, Chengdu 610041, P. R. China, E-mail: 397461170@qq.com

Copyright © 2019, Northwest Institute for Nonferrous Metal Research. Published by Science Press. All rights reserved.

1 Experiment

All samples were synthesized through the solid-state reaction method. Components were chosen according to the chemical formula $\text{Sr}_{0.3}\text{La}_{0.3}\text{Ca}_{0.4}\text{Fe}_{10.625}\text{Co}_{0.225}\text{Zn}_{0.1}\text{O}_{19}$. All the precursor materials of SrCO_3 , CaCO_3 , La_2O_3 , Fe_2O_3 , Co_2O_3 and ZnO were powders of analytical grade. Firstly, these powders were mixed and presintered at 1250°C for 2 h in air atmosphere. Then the presintered samples were further wet-milled for 4 h. The finely milled slurry was compacted into disk-shaped pellets under 8 MPa in the magnetic field of 1000 kA/m, and then calcined at 1200°C for 2 h in air.

Phase composition of the samples used in this paper was analyzed by X-ray diffraction and high-temperature X-ray diffraction (HTXRD) in a θ - 2θ diffractometer using $\text{Cu-K}\alpha$ radiation. The thermal analysis was carried out in a simultaneous thermogravimetric analysis and differential scanning calorimetry (TG-DSC) under air atmosphere. The surface morphology and microstructure of the sintered magnets was observed by a field emission scanning electron microscope (FE-SEM). Magnetic property measurements at room temperature were performed in a vibrating sample magnetometer (VSM) up to 1.9 T.

2 Results and Discussion

2.1 Thermal analysis

As in Fig.1, the TG-DSC curves can be divided into four parts.

2.1.1 Dehydration

There is a small endothermic peak at 379°C , accompanied by the mass loss of 1.34% in the TG-DSC. This stage should be the decomposition of La_2SrO_x ($2\text{La}(\text{OH})_3\text{-SrCO}_3$)^[11]. It is due to the combination of SrCO_3 and $\text{La}(\text{OH})_3$ generated by La_2O_3 and water ionization in the wet grinding process. Fig.2 shows the characteristic peak of La_2SrO_x vanishes after the

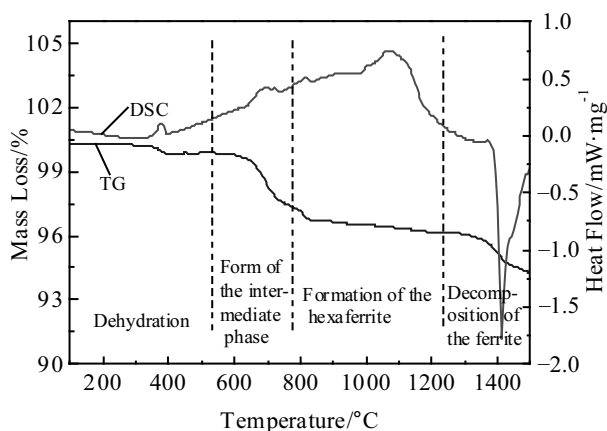


Fig.1 TG and DSC curves of $\text{Sr}_{0.3}\text{La}_{0.3}\text{Ca}_{0.4}\text{Fe}_{10.625}\text{Co}_{0.225}\text{Zn}_{0.1}\text{O}_{19}$ at the heating rate of $10^\circ\text{C}/\text{min}$

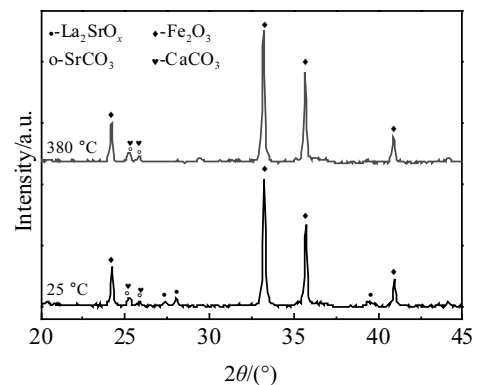
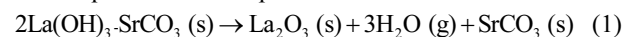


Fig.2 HTXRD patterns of $\text{Sr}_{0.3}\text{La}_{0.3}\text{Ca}_{0.4}\text{Fe}_{10.625}\text{Co}_{0.225}\text{Zn}_{0.1}\text{O}_{19}$ at 380°C for 30 min

sintering at 380°C for 30 min. Therefore, the HTXRD and TG-DSC show that La_2SrO_x dehydrate endothermally at about 379°C , and combined with the previous research^[11] the reaction equation can be represented as:

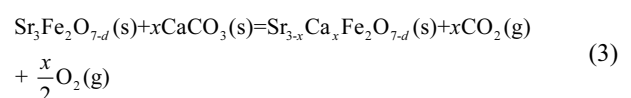
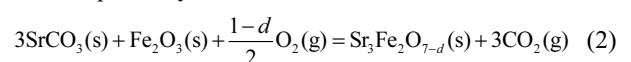


Fossdal^[12] et al observed that impure SrCO_3 decomposed between 350°C and 450°C in TG-DSC test. However, no the reduction of SrCO_3 and the formation of SrO were observed through XRD in this experiment. In addition, the SrCO_3 crystal changed at about 900°C , and then began to decompose^[13]. So, the endothermic reaction is due to La_2SrO_x decomposition at 380°C instead of SrCO_3 .

2.1.2 Formation of intermediate phase

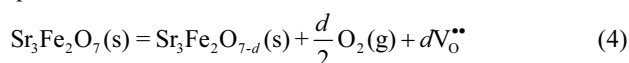
The TG-DSC curves show three consecutive exothermic peaks with a mass loss up to 2.94% between 600°C and 800°C . The characteristic peak of $\text{Sr}_3\text{Fe}_2\text{O}_{7-d}$ appears at 600°C , which becomes clear and sharp with the increasing temperature (Fig.3). Meanwhile the characteristic peaks of SrCO_3 and CaCO_3 gradually disappear. There are mainly Fe_2O_3 and $\text{SrFe}_{12}\text{O}_{19}$ when the calcination temperature increases up to 800°C . At the same time, the XRD does not detect doped Co_2O_3 and ZnO because their contents are too low.

It can be seen that two exothermic peaks exist at 701°C and 721°C on the TG-DSC curve which should be attributed to the formation of the ferrite intermediate phase $\text{Sr}_3\text{Fe}_2\text{O}_{7-d}$ and CaCO_3 dissolving into the $\text{Sr}_3\text{Fe}_2\text{O}_{7-d}$ crystal lattice considering the HTXRD analysis. The equations are as follows respectively:



The influence of the atmosphere sintering on the magnetic properties of the ferrite has been studied. This stage also

illustrates the importance of sintering to the formation of ferrite in an oxygen-containing atmosphere. The inset in Fig.3 shows the $Sr_3Fe_2O_{7-d}$ characteristic peak not only becomes sharp and obvious, but also changes its oxygen stoichiometry with the temperature rise from 600 °C to 750 °C. It is mainly $Sr_3Fe_2O_{7-d}$ in 600 °C, subsequently some $Sr_3Fe_2O_{6.93}$, $Sr_3Fe_2O_{6.74}$, $Sr_3Fe_2O_{6.64}$, $Sr_3Fe_2O_{6.58}$ and $Sr_3Fe_2O_6$ are found between 680 °C and 750 °C. It is shown that the oxygen vacancies ordered structures phase $Sr_3Fe_2O_{7-d}$ appears during the heating process. With the temperature increasing, some tetravalent iron transforms into trivalent iron and the corresponding oxygen vacancies appear, which can be expressed as:



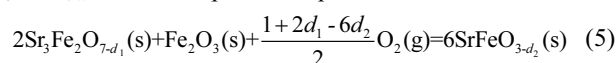
For $d=1$, all Fe is reduced to the trivalent state.

The perovskite $SrFeO_{3-d}$ also belongs to the RP type compound, and about oxygen vacancies ordered structures were studied. Some studies have shown that the stoichiometry of oxygen is a function of temperature and partial pressure of oxygen^[14,15]. Like $SrFeO_{3-d}$, the oxidation state of $Sr_3Fe_2O_{7-d}$ is related to temperature and partial pressure of oxygen, as well as affects its magnetic properties and crystal structure. The point defect reaction is accompanied by a continuous endothermic enthalpy and mass loss due to the formation of O_2 . It can be seen that there are three thermal reactions between 600 °C and 860 °C from the TG-DSC curve in Fig.1. The second thermal reaction should be finished at about 740 °C. There is, however, no $SrFe_{12}O_{19}$ by XRD after annealed at 760 °C for 3 h, so the continuous endotherm and mass loss before 820 °C indicate the formation of $SrFe_{12}O_{19}$ and the formation of oxygen vacancies ordered structures of $Sr_3Fe_2O_{7-d}$. It is confirmed that the average stoichiometric

number of oxygen in $Sr_3Fe_2O_{7-d}$ is 6.27 before $SrFe_{12}O_{19}$ generated.

Beppu^[16] found that only oxygen ions in the 2a site are eliminated by the H_2 reduction. In addition, the perovskite double layer of $Sr_3Fe_2O_7$ allows ordering of the oxygen vacancies by total removal of the oxygen linking the octahedral layers^[12]. Therefore, the formation of point defects may depend strongly on the lattice sites. And it is likely that such a structure is more favorable to its stability at high temperatures.

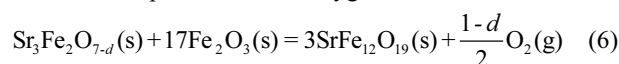
The perovskite $SrFeO_{3-d}$ was obtained by annealing at 750 °C for 30 min, which is different from the result obtained by HTXRD. This may be because $SrFeO_{3-x}$ is easy to decompose in the annealing process due to the poor thermal stability of $Sr_3Fe_2O_{7-x}$. The decomposition equation is as follows:



At the same time, $Sr_{1-x}La_xFeO_{3-d}$ is also found. It indicates that La^{3+} may have dissolved into the $Sr_3Fe_2O_{7-d}$ lattice at more than 700 °C. Martinez^[17] obtained $SrFeO_{3-d}$ during the reduction of $SrFe_{12}O_{19}$ by H_2 . If $SrFe_{12}O_{19}$ can decompose to perovskite, it is possible that $Sr_3Fe_2O_{7-d}$ as the intermediate phase of $SrFe_{12}O_{19}$ decompose to $SrFeO_{3-d}$. On the other hand, the $SrFe_{12}O_{19}$ magnetoplumbite nanofibers ferrite of low-temperature is composed of metastable atomic clusters of many kinds of atomic arrangement with some intrinsic connections^[18]. This metastable atomic clusters can form different crystal (the intermediate phase) under different thermodynamic conditions. This may be, therefore, a reason that different intermediate phase was found in previous studies.

2.1.3 Formation of ferrite

Fig.1 shows a large endothermic peak around 820 °C with a further decrease in mass. It can be seen that $Sr_3Fe_2O_{7-d}$ gradually disappears and M phase appears in Fig.3, indicating that the Sr-rich phase $Sr_3Fe_2O_{7-d}$ with the excess Fe_2O_3 further react to form M phase and emit oxygen:



In previous studies^[12], $SrCO_3$ first decomposes to SrO at low temperature, and SrO reacts with Fe_2O_3 to form magnetoplumbite ferrite through a series of reactions. Based on the above discussion, it is known that $SrCO_3$ can react directly with Fe_2O_3 , and does not need to decompose into transition phase SrO to further react with Fe_2O_3 .

It can be seen that the DSC curve is asymmetric, with relatively wide endotherm peak at 1060 °C from the Fig.1. While the TG curve tends to be stable, and there is no sign of mass change. It is known through XRD that the endothermic peak corresponds to crystallization of amorphous strontium hexaferrite. Gajbhiye^[19] also found a endothermic peak of crystallite after the formation of $SrFe_{12}O_{19}$, in agreement with our experiment. The amorphous strontium hexaferrite is

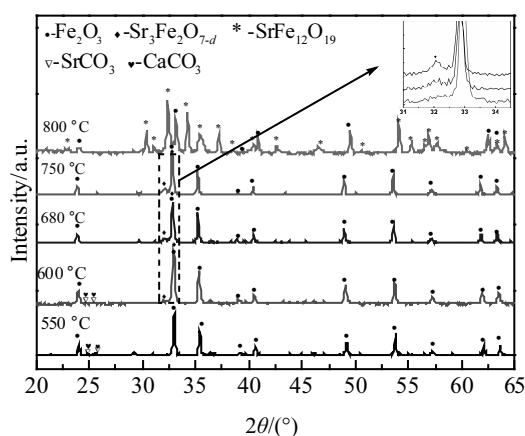


Fig.3 HTXRD patterns of $Sr_{0.3}La_{0.3}Ca_{0.4}Fe_{10.625}Co_{0.225}Zn_{0.1}O_{19}$ at different temperatures for 30 min (the inset is the partial enlargement of 2θ at 32°)

destabilized and easy to decompose at low temperatures. The continuous endotherm with increasing temperature may be due to the fact that dopants (Ca^{2+} , La^{3+} , Co^{3+} , Zn^{2+}) gradually homogeneously dissolve into the $\text{SrFe}_{12}\text{O}_{19}$ crystal lattice above 800 °C. It is also seen that $\text{SrFe}_{12}\text{O}_{19}$ is already perfectly crystalline with a high single degree at 1190 °C according to the XRD patterns, SEM micrographs and EDS analysis of the annealed samples in Fig.4 and 5, and the dopants are evenly distributed in the crystal lattice. The Eqs. (2) and (6) also illustrate that Sr-excess is beneficial to the absorption of Fe_2O_3 . On the other hand, it also shows that SrO has a certain solubility in $\text{SrFe}_{12}\text{O}_{19}$, and $\text{SrFe}_{12}\text{O}_{19}$ has phase width in the pseudo-binary $\text{SrO-Fe}_2\text{O}_3$ system.

2.1.4 Decomposition of the ferrite

In Fig.6a, samples annealed for 2 h in air display a continuous increase of shrinkage rate with the temperature rise. This shrinkage behavior is also reflected in the densification of green compacts, and conducive to the improvement of remanence. The shrinkage rate of magnet with Sr-excess ($\text{Sr}_{0.3}\text{La}_{0.3}\text{Ca}_{0.4}\text{Fe}_{10.625}\text{Co}_{0.225}\text{Zn}_{0.1}\text{O}_{19}$) is higher than that of magnet with stoichiometric M-type ferrite ($\text{Sr}_{0.3}\text{La}_{0.3}\text{Ca}_{0.4}\text{Fe}_{11.675}\text{Co}_{0.225}\text{Zn}_{0.1}\text{O}_{19}$) after 1040 °C, which may be due to forming liquid phase with Sr-excess. Additionally, Langhof^[20] found that the magnet of Sr-excess shrinks sharply at 1206 °C, which proves that the excessive SrO can promote the density of magnet because of the formation of liquid phase. So, the proper excess of strontium is conducive to sintering. It is difficult to observe the differentiation of these compounds by the BSE images because the elements of the ferrites and

Sr-rich phase are similar. Fig.1 shows that a large exothermic peak appears accompanied by mass loss of 1.64% at about 1380 °C. Previous research^[20,21] showed that a series of mass losses and three endothermic DTA signals are observed in the study of Fe-rich part of the pseudo-binary system $\text{SrO-Fe}_2\text{O}_3$ through TG-DTA. The first DTA peak with an onset of 1418 °C indicates the incongruent melting of $\text{SrFe}_{12}\text{O}_{19}$ and formation of X-type ferrite when Fe:Sr=12:1, and a mass loss of 0.5% is indicative of the reduction process. The second peak (onset at 1435 °C) represents the melting of the X-type

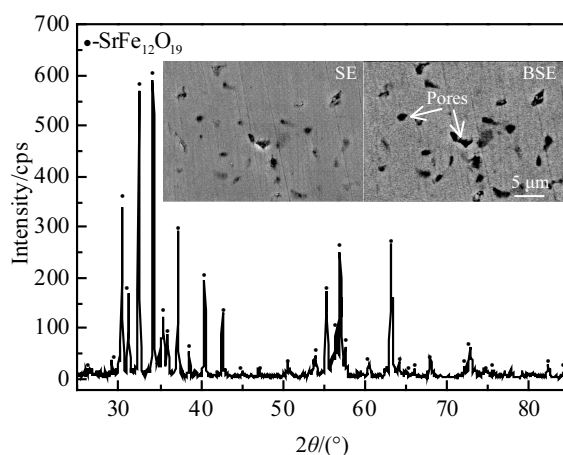


Fig.4 XRD patterns and SEM micrographs of $\text{Sr}_{0.3}\text{La}_{0.3}\text{Ca}_{0.4}\text{Fe}_{10.625}\text{Co}_{0.225}\text{Zn}_{0.1}\text{O}_{19}$ sintered at 1190 °C for 2 h

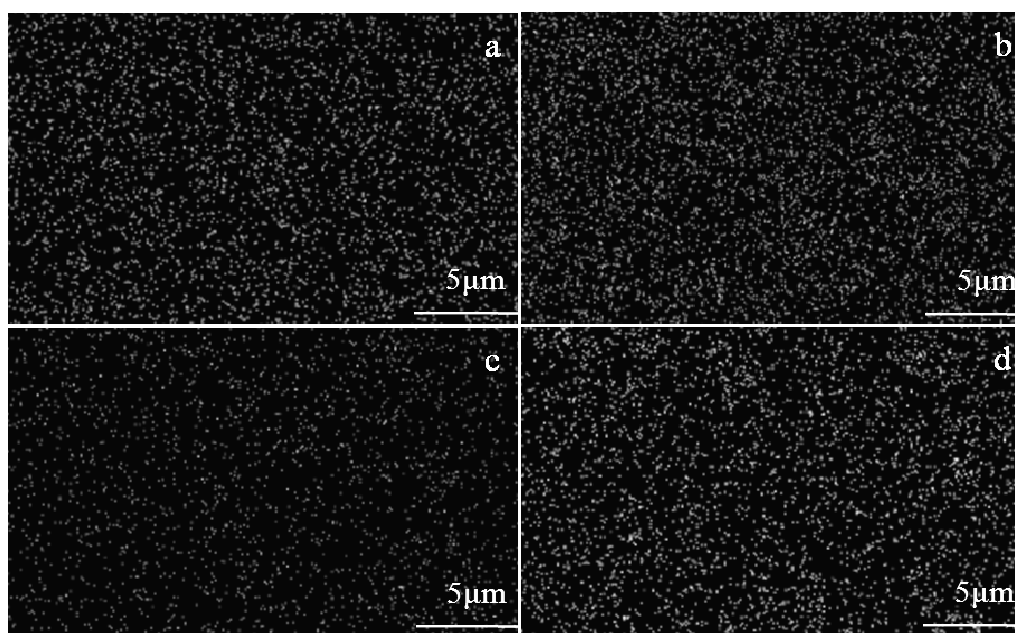


Fig.5 EDS mapping of La (a), Ca (b), Co (c) and Zn (d)

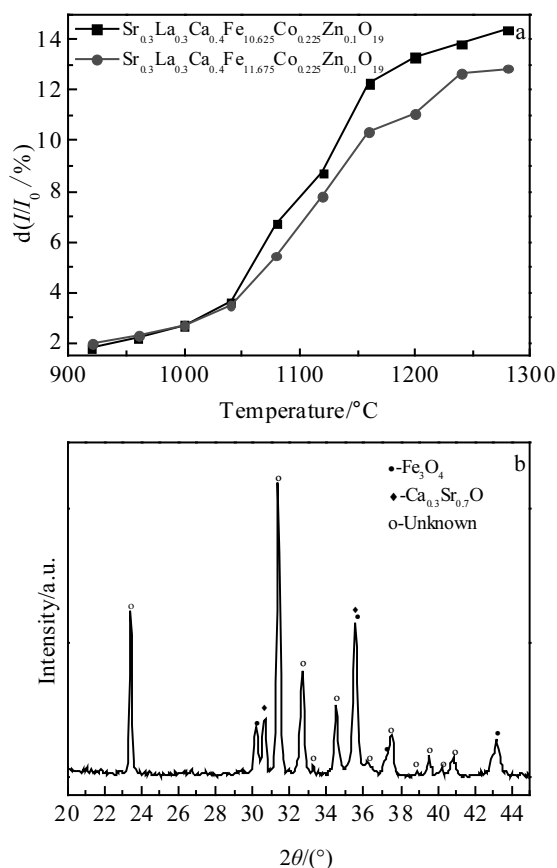


Fig.6 Shrinkage rate curves of $\text{Sr}_{0.3}\text{La}_{0.3}\text{Ca}_{0.4}\text{Fe}_{10.625}\text{Co}_{0.225}\text{Zn}_{0.1}\text{O}_{19}$ and $\text{Sr}_{0.3}\text{La}_{0.3}\text{Ca}_{0.4}\text{Fe}_{11.675}\text{Co}_{0.225}\text{Zn}_{0.1}\text{O}_{19}$ (a); XRD patterns of $\text{Sr}_{0.3}\text{La}_{0.3}\text{Ca}_{0.4}\text{Fe}_{10.625}\text{Co}_{0.225}\text{Zn}_{0.1}\text{O}_{19}$ annealed at 1450 $^{\circ}\text{C}$ for 2 h (b)

ferrite and formation of W-type hexagonal ferrite, and a mass loss of 0.3% is observed. The third peak (onset at 1452 $^{\circ}\text{C}$) finally signals the incongruent melting of W-type ferrite and formation of magnetite with a corresponding mass loss of 1.0%. There is no continuous phase transition in the high temperature region in Fig.1, and a large amount of liquid phase, Fe_3O_4 , $\text{Ca}_{0.3}\text{Sr}_{0.7}\text{O}$ and unknown products are found at 1450 $^{\circ}\text{C}$ as Fig.6b. The TG-DSC curve in this study is similar to the TG-DTA curve of $\text{Sr}_{1-x}\text{La}_x\text{Fe}_{12}\text{O}_{19}$ ($x=0.25, 0.5, 0.75$) from study by Seifert of the La substituted M strontium hexagonal ferrite^[22]. Combined with this study, M phase may generate an unknown phase at high temperature and may also be the X-type ferrite decomposed into unknown phase because of poor thermal stability.

2.2 Magnetic properties

It can be observed from Fig.7 that the rectangularity of the demagnetizing curves of LaCaCoZn-type substituted ferrite powder decreases compared to that of unsubstituted ferrite powder. Previous research^[23,24] has shown the Co^{3+} ions substituted for Fe^{3+} ions in the octahedral $4f_2$ and 2a sites,

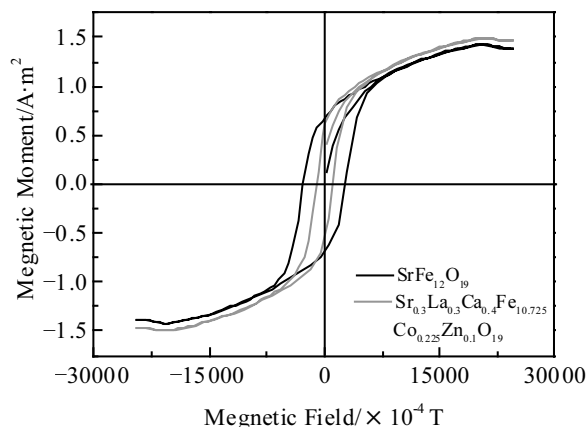


Fig.7 Magnetic hysteresis loops of the M-type ferrite powders

besides a valence change of some Fe^{3+} to Fe^{2+} in the 2a site. The introduction of Co^{2+} and La^{3+} is beneficial to magnetic properties due to the special electronic structure of the substituted ions and their preference occupying in the magnetic cell. In particular, the addition of La-Co significantly improves the anisotropy-crystalline anisotropy field^[25]. The non-magnetic Zn^{2+} ions preferentially substitute Fe^{3+} ions in $4f_1$ site and decrease the magnetic moment in the spin-down direction^[26]. On the other hand, as the $4f_1$ site is in the close vicinity of the 2a site, the substitution of some Fe^{3+} ion by the nonmagnetic Zn^{2+} ion in $4f_1$ site induces a perturbation of the 2a site. This may cause an increase of the superexchange $4f_1\text{-O}^{2-}\text{-2a}$ interactions^[26,27]. So, the addition of Zn^{2+} can be attributed to the increase of the saturation magnetization. But the addition of Zn^{2+} greatly reduces the anisotropy-crystalline anisotropy field, which is harmful to the coercive force^[28]. It is well known for the M-type hexaferrites that the intensity of superexchange interaction is thought to associate with the magnetic moment of M, the M-O distance and the M-O-M angle (M represents transition-metal). By substitution of La^{3+} ions and Ca^{2+} ions, the lattice constant c may have been decreased because the radius of Ca^{2+} ion (0.106 nm) and the radius of La^{3+} ion (0.122 nm) is smaller than that of Sr^{2+} ion (0.132 nm)^[29,30]. This results in the enhancement of the $\text{Fe}^{3+}\text{-O}^{2-}\text{-Fe}^{3+}$ superexchange interaction strength. In addition, Liu showed enlarged hyperfine fields for the 12k- and 2b-sites, such an increase of the exchange interaction of the Fe^{3+} ion at the 12k- and 2b-lattice sites^[29,30]. They are conducive to the improvement of remanence. As can be seen from Fig.8, the particle size of LaCaCoZn-type substituted ferrite powder increases obviously and grains morphology changes from hexagonal to lath-shaped. Such changes in grain morphology are detrimental to coercivity. This may be related to the addition of Ca^{2+} ions^[31].

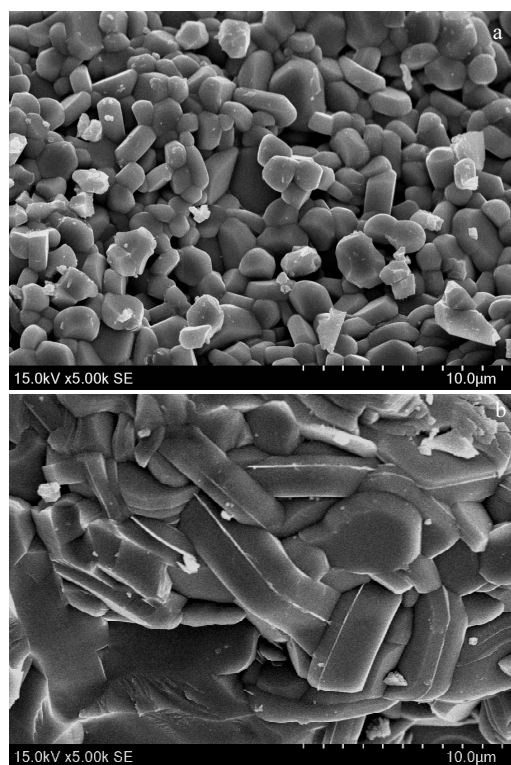


Fig.8 SEM micrographs of the M-type ferrite SrFe_{11.05}O₁₉ (a) and Sr_{0.3}La_{0.3}Ca_{0.4}Fe_{10.625}Co_{0.225}Zn_{0.1}O₁₉ (b)

3 Conclusions

1) The La₂SrO_x appears in the preparation process and dehydrates at about 380 °C.

2) The formation of magnetoplumbite-type ferrite in air has two steps: SrCO₃ and Fe₂O₃ first generate the intermediate phase Sr₃Fe₂O_{7-d} around 700 °C. And then Sr₃Fe₂O_{7-d} and the remaining unreacted Fe₂O₃ generate SrFe₁₂O₁₉. At the same time, La³⁺ and Ca²⁺ also dissolve into the intermediate phase to form Sr_{3-3x-y}La_xCa_yFe₂O_{7-d}.

3) The perovskite SrFeO_{3-d} is obtained by annealing at 750 °C.

4) The shrinkage rate of magnet with Sr-excess is higher than that of magnet with stoichiometric M-type ferrite after 1040 °C, which may be due to liquid phase formation because of Sr-excess.

5) The rectangularity of the demagnetizing curves of LaCaCoZn-type substituted ferrite powder decreases compared to that of unsubstituted ferrite powder. The saturation magnetization is improved due to the addition of Zn²⁺.

References

- Batti P. *Ceramurgia*[J], 1976, 6: 11
- Fossdal A, Einarsrud M A, Grande T. *Journal of Solid State Chemistry*[J], 2004, 177(8): 2933
- Lucchini E, Slokar G. *Journal of Magnetism & Magnetic Materials*[J], 1980, 21(1): 93
- Fossdal A, Einarsrud M A, Grande T. *Journal of the American Ceramic Society*[J], 2010, 88(7): 1988
- Yang Y J, Liu X S, Jin D L. *Materials Science & Engineering B*[J], 2014, 186(1): 106
- Xu Y F, Ma Y Q, Zhang X et al. *European Physical Journal Applied Physics*[J], 2013, 62(1): 777
- Langhof N, Seifert D, Göbbels M et al. *Journal of Solid State Chemistry*[J], 2009, 182(9): 2409
- Haberey F, Kockel A. *IEEE Transactions on Magnetics*[J], 1976, 12(6): 983
- Berbenni V, Marini A. *Materials Research Bulletin*[J], 2002, 37(2): 221
- Beretka J, Brown T. *Australian Journal of Chemistry*[J], 1971, 24(2): 237
- Marques R F C, Zorel H E, Crespi M S et al. *Journal of Thermal Analysis & Calorimetry*[J], 1999, 56(1): 143
- Fossdal A, Einarsrud M A, Grande T. *Journal of Solid State Chemistry*[J], 2004, 177(8): 2933
- Liu X G, Peng X D, Xie W D et al. *Chinese Journal of Materials Research*[J], 2005, 19(3): 288 (in Chinese)
- Takeda Y T T, Kanno K, Takada T et al. *Journal of Solid State Chemistry*[J], 1986, 63(2): 237
- Post M L, Sanders B W, Kennepohl P. *Sensors & Actuators B: Chemical*[J], 1993, 13(1-3): 272
- Beppu K, Hosokawa S, Teramura K. *Journal of Materials Chemistry A*[J], 2015, 3(25): 13 540
- Martinez N, Williams AJ, Ebrahimi S A S et al. *Journal of Materials Science*[J], 1999, 34(10): 2401
- Zhao W Y, Zhang Q J, Li P et al. *Journal of the Chinese Ceramic Society*[J], 2003, 31(1): 20
- Gajbhiye N S, Vijayalakshmi A. *Journal of Thermal Analysis & Calorimetry*[J], 1998, 51(2): 517
- Langhof N, Seifert D, Göbbels M et al. *Journal of Solid State Chemistry*[J], 2009, 182(9): 2409
- Toepfer J, Seifert D, Le Breton J M et al. *Journal of Solid State Chemistry*[J], 2015, 226: 133
- Seifert D, Töpfer J, Langenhorst F et al. *Journal of Magnetism & Magnetic Materials*[J], 2009, 321(24): 4045
- Lechevallier L, Le Breton J M, Teillet J et al. *Physica B: Condensed Matter*[J], 2003, 327(2-4): 135
- Tenaud P, Morel A, Kools F et al. *Journal of Alloys & Compounds*[J], 2004, 370: 331
- Kools F, Morel A, Grössinger R et al. *Journal of Magnetism & Magnetic Materials*[J], 2002, 242-245: 1270
- Lechevallier L, Le Breton J M. *Journal of Magnetism & Magnetic Materials*[J], 2005, 290-291: 1237
- Bao H W, Fang Q Q. *Journal of Magnetic Materials and Devices*[J], 2004, 35(3): 22 (in Chinese)
- Wang F, Chen Z Y, Peng Y et al. *Metallic Functional Materials*[J], 2015, 22(4): 25 (in Chinese)

- 29 Liu X S, Zhong W, Yang S et al. *Journal of Magnetism & Magnetic Materials*[J], 2002, 238(2-3): 207
- 30 Yang Y J, Wang F H, Shao J X et al. *Journal of Magnetism & Magnetic Materials*[J], 2016, 401: 1039
- 31 Li X, Yang W G, Bao D X et al. *Journal of Magnetism & Magnetic Materials*[J], 2013, 329: 1

La-Ca-Co-Zn 掺杂 M 型锶铁氧体的相变和磁性能

安健樟¹, 叶金文¹, 唐正华¹, 陈一可², 秦 尧³

(1. 四川大学, 四川 成都 610041)

(2. 锦钛精工科技有限公司, 四川 成都 610041)

(3. 西南石油大学, 四川 成都 610500)

摘 要: 采用陶瓷法制备 La-Ca-Co-Zn 掺杂的 M 型锶铁氧体 $\text{Sr}_{0.3}\text{La}_{0.3}\text{Ca}_{0.4}\text{Fe}_{10.625}\text{Co}_{0.225}\text{Zn}_{0.1}\text{O}_{19}$ 。使用高温 X 射线衍射仪、振动样品磁强计、热分析和扫描电子显微镜等对 $\text{Sr}_{0.3}\text{La}_{0.3}\text{Ca}_{0.4}\text{Fe}_{10.625}\text{Co}_{0.225}\text{Zn}_{0.1}\text{O}_{19}$ 在 25 °C 到 1450 °C 的相变过程进行了分析, 并且讨论了其磁性能。结果表明: La-Ca-Co-Zn 掺杂的 M 型六方铁氧体的形成主要分为 2 个部分, 在 700 °C 左右, SrCO_3 和 Fe_2O_3 先反应生成中间相 $\text{Sr}_3\text{Fe}_2\text{O}_{7-d}$, 然后 $\text{Sr}_3\text{Fe}_2\text{O}_{7-d}$ 再和剩下的 Fe_2O_3 反应生成 M 相, 并且 $\text{Sr}_3\text{Fe}_2\text{O}_{7-d}$ 中的 Fe 离子化合价与温度有关; 随着温度升高, La^{3+} , Ca^{2+} , Co^{2+} 和 Zn^{2+} 开始逐渐溶入中间相或者随后生成的 M 相中, 且在 M 相中分布均匀; 和高温射线衍射仪检测结果不同的是在 700 °C 左右退火时, 得到了钙钛矿相; 在 1200 °C 烧结, 可以得到单一程度很高的 M 相, 但有少量的第二相存在, 第二相的存在有利于提高烧结致密度; 当烧结温度为 1380 °C 时, 铁氧体开始分解; $\text{Sr}_{0.3}\text{La}_{0.3}\text{Ca}_{0.4}\text{Fe}_{10.625}\text{Co}_{0.225}\text{Zn}_{0.1}\text{O}_{19}$ 铁氧体粉末退磁曲线的矩形度要低于 SrFeO_{12} 的退磁曲线矩形度。

关键词: 中间相; 相变; 磁性能; 热分析

作者简介: 安健樟, 男, 1992 年生, 硕士, 四川大学材料科学与工程学院, 四川 成都 610041, E-mail: 245155367@qq.com